http://dx.doi.org/10.21611/qirt.2004.014

Automatic Interpolated Differentiated Absolute Contrast Algorithm for the Analysis of Pulsed Thermographic Sequences

by D. A. González*, C. Ibarra-Castanedo**, M. Pilla**, M. Klein**, J.M. López-Higuera*, X. Maldague**.

** Universidad de Cantabria, Grupo de Ingeniería Fotónica, Avda. Los Castros s/n, 39005 Santander (Cantabria) Spain, E-mail: dagonfer@teisa.unican.es*
*** Universitè Laval, Quebec City (Quebec) G1K7P4, Canada*

Abstract

An automation of the Differentiated Absolute Contrast (DAC) method, called Interpolated Differentiated Absolute Contrast Algorithm (IDAC), is proposed for pulsed infrared thermography. Based on the previously known method, the new algorithm simplifies the analysis process of thermographic sequences resolving the decisions that the user should normally take when applying the DAC method. The algorithm has been successfully checked experimentally with results obtained using Plexiglas^{TM}, graphite-epoxy and aluminium specimens.

1 Introduction

Non-destructive testing is one of the most useful techniques to implement in quality control process. Nowadays, quality has become one of the most important inducements of any product and its control means a huge investment in production lines. The Thermography is one of the several techniques that can be included into the field of non-destructive testing and which is applied to numerous quality processes. Herein, the Pulsed Thermography (PT) is a procedure commonly used due to the possibility of detecting the presence of a subsurface defect fast. Basically, the PT consists in the exposition of a specimen to a thermal stimulation pulse, which lasts from a few milliseconds to a few seconds depending on the conductivity of the specimen under inspection, and the study of the temperature decay after such exposition [1].

Among thermogram processing techniques, thermal contrast is often employed for enhancing subsurface defects detection, image quality and even for obtaining some quantitative approximations regarding the depth, thermal properties and size of the defects. The different contrast definitions require the identification of a non-defective zone or “sound area” or, better, the cold image, and this is often a limitation because it demands a priori knowledge of the specimen. The definition of the sound area becomes a critical issue and, because it will always be an assumption, this is a strong limitation that provides inaccuracy to contrast methods [2]. Some attempts have been proposed for avoiding this necessity of sound area knowledge and, even, overcoming other problems such as the non-uniformity of the thermal stimulation or the tilt of the heat pulse source respected to the normal to the specimen surface. Among them, the Differentiated Absolute Contrast (DAC) method is one of the simplest and easily implemented [3]. However, the experience of an operator working in this field still is necessary in order to obtain satisfactory results and clear contrast images.

http://dx.doi.org/10.21611/qirt.2004.014

In this paper, an automation of the DAC method is proposed to overcome this necessity of human control. First of all, a theoretical background of the thermal conduction model used by this method is described. Then, a review of the DAC method leads to the presentation of the proposed algorithm for enhancing of contrast images without any human intervention. Last sections show the results and conclusions resulting from experiments testing different specimens from different materials.

2 Theoretical background

The theoretical simulation of the transient heat flow in a body follows the three-dimensional differential equation called Fourier diffusion equation. This equation is a general expression of the conservation of energy for a medium in which heat is generated and propagated and can be expressed as [4]:

$$\nabla \cdot \left[k \nabla \mathrm{T}(r,t)\right] + g(r,t) = \rho C_p \frac{\partial \mathrm{T}(r,t)}{\partial t} \tag{1}$$

where *k* is the thermal conductivity in W/(m·K), $T(r,t)$ is the temperature distribution as a function of position and time, ***g(r,t)*** is the rate of energy generation per unit volume in the medium (W·m^3) and *C* and ρ the specific heat (J·kg^{-1}·K^{-1}) and the density (kg·m^{-3}) of the material.

Assuming that the specimens under test are homogeneous, in a defect free sample at a point far from any edge, lateral heat components cancel and the simplest model used to solve equation 1, assuming a Dirac thermal pulse is been applied to the body, can be expressed by:

$$\Delta \mathrm{T}_{semi-\inf inite-body}(z=0,t) = \frac{Q}{e\sqrt{\pi t}} \tag{2}$$

where ***z*** is the depth variable (***z****=0* corresponds to the surface), *Q* is the injected energy at the surface in J/m^2, ***e*** is the thermal effusivity ($e = \sqrt{k\rho C_p}$) and ΔT is the temperature increase from ***t****=0*.

Considering *t'* as a time comprised between the time of flash impulse (*t_0)* and the time at which the first defect becomes visible [3],

$$\Delta T_{soundarea[i,j]}(t') = \Delta T_{[i,j]}(t') = \frac{Q_{[i,j]}}{e_{[i,j]}\sqrt{\pi t'}} \tag{3}$$

Applying this model, the temperature of a free-of-defects area can be obtained for each time. Moreover, if the injected energy is assumed to change relatively smoothly, ***Q/e*** can be solved locally and the following relation can be extracted [3]:

$$\Delta T_{soundarea[i,j]}(t) = \frac{Q_{[i,j]}}{e_{[i,j]}\sqrt{\pi t}} = \frac{\sqrt{\pi t'}}{\sqrt{\pi t}} \Delta T_{[i,j]}(t') = \sqrt{\frac{t'}{t}} \Delta T_{[i,j]}(t') \tag{4}$$

Solving the last equation for all the locations over the surface, a whole temporal sequence of the reconstructed "ideal" defect-free specimen is obtained.

2.1 DAC method

Combining the precedent model with the well-known absolute thermal contrast definition [1]:

$$C_{AC[i,j]}(t) = T_{[i,j]}(t) - T_{soundarea}(t) \tag{5}$$

http://dx.doi.org/10.21611/qirt.2004.014

The DAC method, as a generalization of the absolute contrast definition, applies the following relation for each location [3]:

$$C_{DAC[i,j]}(t) = \Delta T_{[i,j]}(t) - \Delta T_{soundarea[i,j]}(t) = \Delta T_{[i,j]}(t) - \sqrt{\frac{t'}{t}}\Delta T_{[i,j]}(t') \qquad (6)$$

where

$$\begin{aligned} \Delta T_{[i,j]}(t) &= T_{[i,j]}(t) - T_{[i,j]}(0^-) \\ T_{[i,j]}(0^-) &= T_{soundarea[i,j]}(0^-) \end{aligned} \qquad (7)$$

Therefore, the DAC method provides advantages such as the no need to make assumptions on the sound areas localization and the possibility of computing a local $T_{soundarea[i,j]}(t)$ even in not evenly heated surfaces. Interestingly, reference [5], proposed earlier, also discussed on updating the contrast method. However, some further improvements maybe provided to the DAC method. Up to now, both determining of the initial time *t'* as well as establishing the best agreement with the "ideal" slope of –0.5 for a free-defect area has been left to the user. These issues always give some uncertain results, mainly taking into account that subjectivity is always involved in human criterion. The algorithm proposed below, resolves these issues enhancing at the same time the results found by the DAC method.

3 IDAC method

An automation of the DAC method is proposed here, making the process of contrast optimization independent of operator and instead basing it on several mathematical certainties.

For each pixel, the developed algorithm can be summarized in the following steps:

- Identify, among the temporal evolution data, the first point having a slope greater than a given threshold (-0.35 has been used based on experience). That point in the curve could be interpreted as the beginning in the detection of a defect (defect's point).
- From the first point of data up to the defect's point, a search of the optimization point is run. Basically, the optimization point is that which has a closest to -0.5 slope in fitting the curve among itself, the next point and the following one, in the logarithmic scale representation.
- Once the optimization point is found, the points in the temporal range $[t_0, t_{optimization\ point}]$ are compared with those obtained applying the coefficients of the power regression (line in the logarithmic scale). A minimization function has been implemented for getting the optimal epsilon which, added to the temporal axis, best fit the t_0 value. In this way, a good $Q/e_{[i,j]}$ estimation could be obtained.

In order to check the developed IDAC algorithm, several experiments were done. In next section, the results obtained for each specimen under test are shown.

4 Experimental Results

Several specimens are used for evaluating the validity of this algorithm. In each subsection, we compare the results obtained by DAC method with those obtained by IDAC. For all tests, specimens were stimulated during 15 ms using two photographic flashes (Balcar FX60), and the thermographic data were recorded using a Santa Barbara focal plane infrared camera, model SBF125.

http://dx.doi.org/10.21611/qirt.2004.014

4.1 Plexiglas TM plate

The first specimen under test is a 4 mm-thick plate made of Plexiglas TM which contains 6 flat-bottom circular holes of 10 mm of diameter and which are localized at different depths (1, 1.5, 2, 2.5, 3, 3.5 mm) (see Figure 1). After the heating pulse, 200 thermograms were recorded (from t=0.1 to t=20 s).

What can be observed on Figure 2 is the plot of the temporal evolution of temperature for some pixels on specimen 1 (shown on Figure 1). The crosses correspond to raw temperature, the dot lines have a –0.5 slope with origin in the first point of each series (DAC) once corrected t_0, and the dash and dot lines are the automatic approximate lines for each case (IDAC). The values shown within the figures are the slopes of the approximate lines at the points of optimization. Excellent agreement can be observed between both methods.

In the Figure 3, the absolute contrast images are presented following the DAC method or this automated method (IDAC). Again, an excellent agreement leads to verify that the automated decisions are similar to qualified operator decisions as can be extracted of the result of computing the correlation coefficient, r, between IDAC and DAC images, $r=0.96$, and comparing the corresponding plotted profiles.

4.2 Graphite-epoxy plate

In this case, the next specimen under test is a 5-ply graphite-epoxy plate. A Teflon TM insert and a thin void space were embedded inside as could be easily seen on Figure 4. Both defects are clearly seen as also possible epoxy-richer zones. The absolute contrast images correspond to 30th thermogram ($t=1.15$ s) of a recorded sequence of 50 thermograms (from t=0.55 to t=1.53 s). The computing of the two-dimensional correlation coefficient between the contrast images gives a value of 0.99 which leads to the conclusion that the same decisions have been used in DAC and IDAC methods.

4.3 Aluminium plate

The last specimen under test is an aluminium alloy plate with 4.76 mm of thickness. It contains 2 concentric circular defects of depth 0.79 and 2.38 mm and diameters of 20.4 and 50.8 mm respectively. After the heating pulse, 50 thermograms were recorded (time for the first frame: 0.080 s, time for the last frame: 1.060 s). In this case, 2D and 3D representations of the absolute contrast image differ due to the fact that the heat conduction in this specimen doesn't follow exactly the Fourier diffusion model for semi-infinite bodies. Given that flat-bottomed holes have been drilled on the specimen, defects are in fact at open-air and the edges are quite near defects areas, so, lateral heat components become predominant. However, these images give some qualitative results respecting to the presence, shape and depth of the defects in spite of the non-flatness of the backgrounds, as it can be observed on Figure 5. The two-dimensional correlation coefficient in this case is 0.99.

5 Conclusions

A new algorithm based on the Differentiated Absolute Contrast (DAC) method is proposed. The Interpolated Differentiated Absolute Contrast (IDAC) algorithm contributes to avoid the necessity of human intervention during the process of getting

http://dx.doi.org/10.21611/qirt.2004.014

the contrast images. More specifically, the particularities of the IDAC are: pixel by pixel computation of a corrected acquisition time, fitting best the –0.5 slope and 1D thermal model assumption.

Experimental works using different materials and plate configurations were realized. The excellent results of the correlation with previous methods validate the proposed IDAC algorithm.

6 Acknowledgements

This work was supported in part by the Spanish Science and Technology Ministry under project SUGAROS TIC2001-0877-C02-01 and also by the Natural Sciences and Engineering Research Council of Canada for what both organizations are thanked.

REFERENCES

[1] Maldague X., Theory and Practice of Infrared Thermography for Nondestructive Evaluation, New York, John Wiley pub., 2001, 684p.

[2] Shepard S.M., “Advances in Pulsed Thermography”, Proc. SPIE: Thermosense XXIII, 4360, 2001, 511-515 p.

[3] Pilla M., Klein M., Maldague X., Salerno A., "New Absolute Contrast for Pulsed Thermography ", QIRT 2002, D. Balageas, G. Busse, G. Carlomagno eds [in Press].

[4] Carlslaw H.S., Jaeger J.C., Conduction of Heat in Solids, Oxford University Press, 2nd edition, 1959.

[5] Martin R. E., Gyekenyesi A. L., Shepard S. M., "Interpreting the Results of Pulsed Thermography Data," Materials Evaluation, 61[5]: 611-616, 2003.

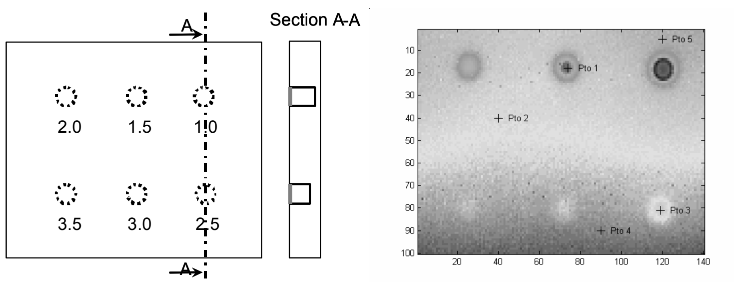

Fig. 1. *a) Scheme of the front (inspected) surface of specimen1. Numbers are the depth of each defect in mm. b) Absolute contrast image of the sequence treated.*

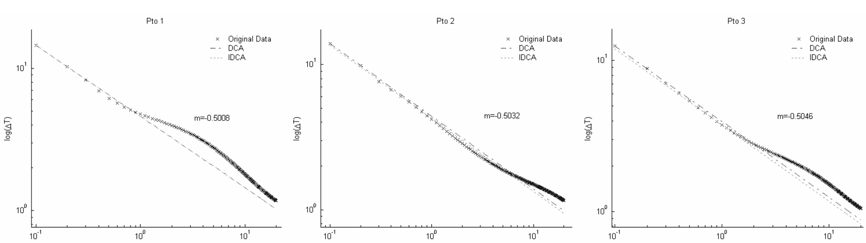

Fig. 2. *Differentiated Contrast evolution versus time for some selected points.*

http://dx.doi.org/10.21611/qirt.2004.014

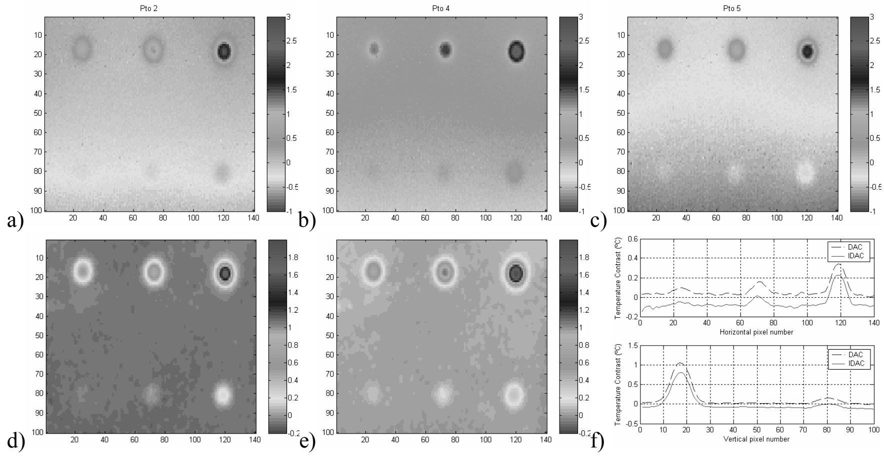

Fig. 3. *Different results for a selected time and the specimen 1. a-c) temperature absolute contrast images taking into account different references (plain vanilla); d,e) IDAC and DAC images with the same scale; f) profiles for a horizontal line at pixel 80 and a vertical line at pixel 72.*

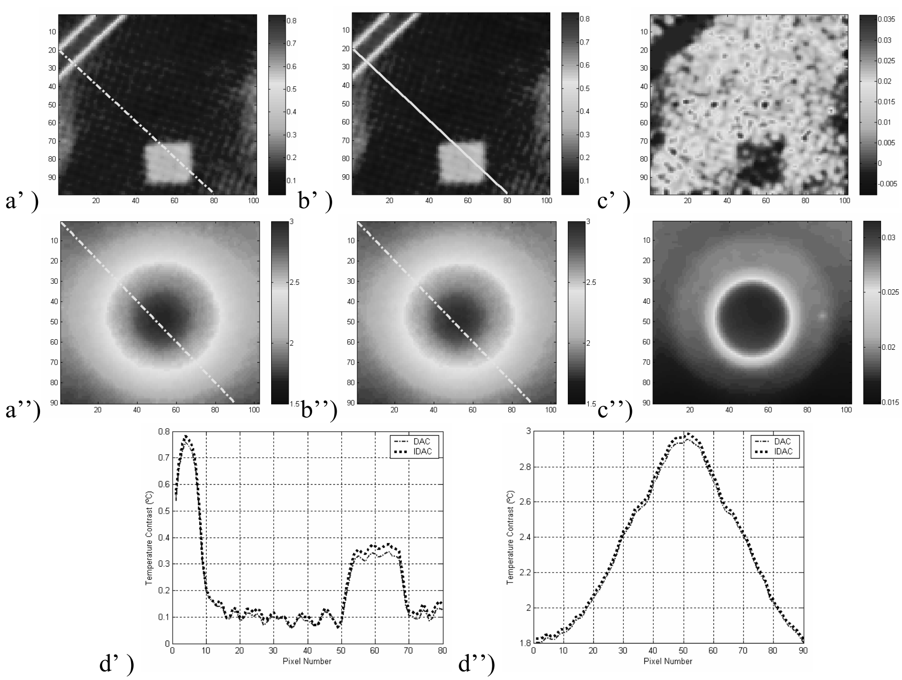

Fig. 4. *Different results for a selected time and the specimens 2 ('graphs) and 3 (''graphs), respectively. a,b) DAC and IDAC temperature absolute contrast images with the same scale; c) difference images between IDAC and DAC images; d) temperature profiles for in-printed lines.*